P10.2 THE DEVELOPMENT AND STRUCTURE OF AN OCEANIC SQUALL LINE SYSTEMS DURING THE SOUTH CHINA SEA SUMMER MONSOON EXPERIMENT

Jian-Jian Wang
Joint Center for Earth System Technology, University of Maryland, Baltimore County, Baltimore, Maryland
Mesoscale Atmospheric Processes Branch, Code 912, NASA/GSFC, Greenbelt, MD 20771

1. INTRODUCTION

The South China Sea Monsoon Experiment (SCSMEX) was conducted in South China Sea (SCS) and surrounding areas during May—June 1998. The primary goal of the experiment is to provide a better understanding of the key physical processes for the onset, maintenance and variability of the monsoon over the Southeast Asia and southern China leading to improved monsoon predictions. The main observing platform during the Intensive Observing Period included two Doppler radars, radiosonde networks, raingauge networks, disdrometers, and ATLAS mooring buoys (Fig. 1). The goals of this study associated with the primary objective are: 1) to document the evolution of an oceanic squall line systems on 24 May 1998, 2) to analyze the rainfall and kinematic structure of the mature phase of the strongest squall line, and 3) to investigate the dynamics of the precipitation processes.

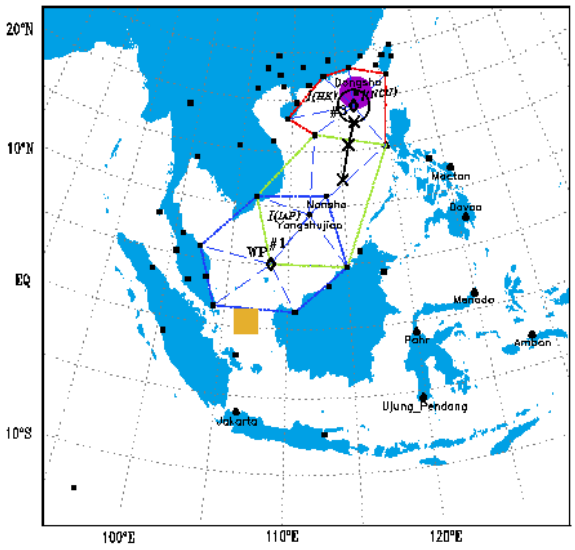

Fig. 1 SCSMEX observing platform.

2. THE EVOLUTION OF THE SYSTEM

The squall line system studied here occurred on 24 May 1998, after the onset of South China Sea summer monsoon during 15-20 May. On 24 May, the observed squall line system was on the east side of a mesoscale convective complex (MCC) embedded in a frontal system from mainland China. The environmental sounding (Fig. 2) showed weak instability with convective available potential energy about 720 J kg^{-1}. The easterly winds dominated the lowest levels with the wind speed of 7-8 m s^{-1}. The winds shifted to westerly at about 800 hPa with a magnitude of 2-3 m s^{-1}. This generated a moderate low-level wind shear of 5.4 x 10^{-3} s^{-1} (about 11 m s^{-1} from 780 to 1000 hPa). The winds from 700 to 250hPa were very weak. In addition, the mid- to upper-level air was quite dry.

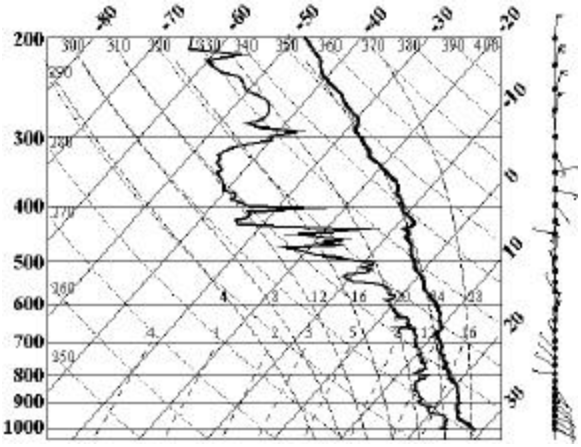

Fig. 2 Sounding launched from research vessel *Shi Yan* #3 at 1200 UTC, 24 May 1998.

The squall line systems included several squall lines persisting from 1200 UTC 24 May to the following day. The early convective echoes appeared at about 1200 UTC in the format of several individual new-formatted convective cells. These small cells lined up to a discontinuous convective line (I) about 50 km west of the CPOL radar (Fig. 3a). The orientation of the convective line was perpendicular to the low-level wind shear (1000 to 800 hPa). On its way moving toward west, this convective line gradually intensified to a broader, stronger, and more organized squall line. From 1200 UTC to 1700 UTC, the northern convective line propagated northwesterly at a speed of 6 to 7 m s^{-1}, which was identical to the maximum low-level wind speed near 800 hPa. This squall line reached its climax both in size and intensity at about 1700 UTC. The peak radar reflectivity was 55 dBZ. The squall line started to dissipate after 1700 UTC. Meanwhile, a new arc-shaped convective line (II) formed about 40 km behind the original squall line. The second convective line became a wider and stronger squall line than the first one in hours later (Fig. 3b). The second squall line reached its climax at about 2200-2400 UTC. The peak reflectivity of 60 dBZ was recorded with the cloud top at about 16 km MSL. The mature squall line started to dissipate around 0400 UTC 25 May (not shown). Another feature during the 10-h period analysis is the third convective line (III). It appeared near 1800 UTC about 80 km behind the second line. The third line enhanced significantly in the next hour or so. However, contrasting the well-

developed second squall line, the third convective line did not reach fully development before its dissipation after 2200 UTC. In general, the squall line system propagated toward northeast at a median average speed of 7-8 m s^{-1}. The northern portion of the system moved somewhat faster and the south portion of the system migrated a bit slower. Comparing to the weak winds at mid-levels from 1200 UTC sounding, the propagating speed of the system was fast.

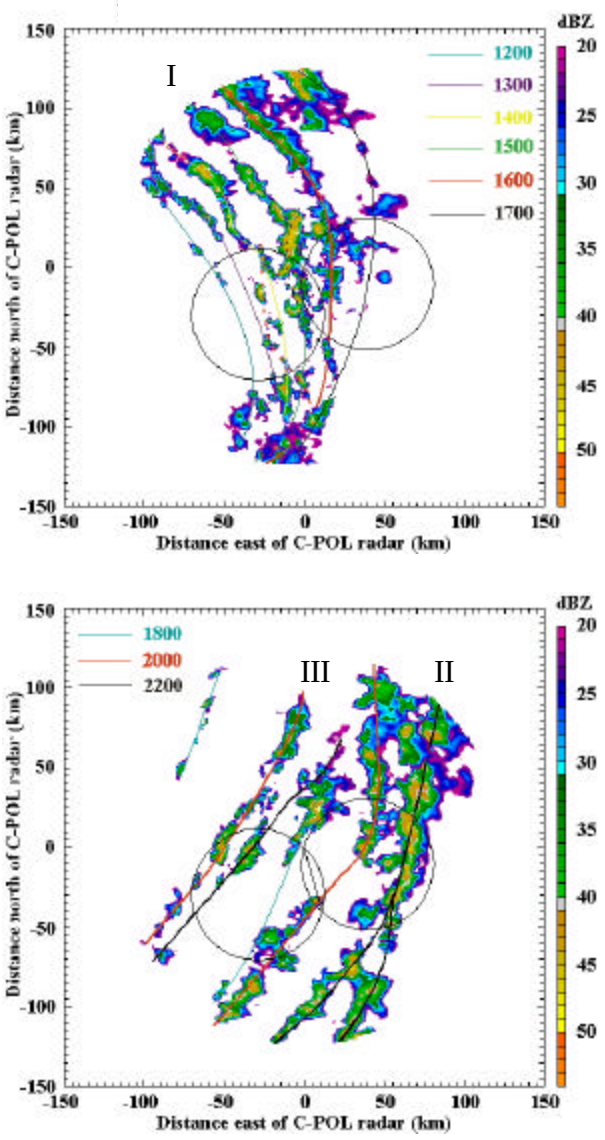

Fig. 3 Radar reflectivity CAPPI at 2km from 1200 to 2200 UTC, 24 May 1998.

3. THE STRUCTURE OF THE SQUALL LINE

Among the three squall lines on 24 May, the squall line II was the strongest. We have performed 3-h dual-Doppler radar analysis from 1900 to 2200 UTC when the main part of the squall line was in the dual-Doppler analysis lobes. In this section, we will discuss the rainfall and kinematic structure of the squall line at 2040 UTC. A more detailed analysis throughout the 3-h period will be presented at the conference.

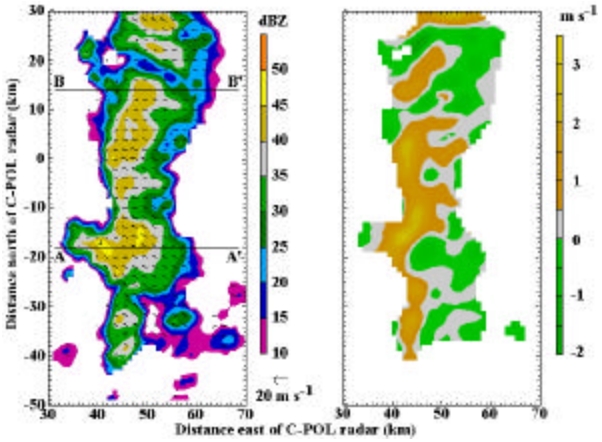

Fig. 4 Horizontal analysis of radar reflectivity and system-relative wind flow (left) and vertical air motion at 1.5 km MSL valid at 2040 UTC.

At 2040 UTC, as shown in Fig. 4, the mature squall line became a continuous rainband in the right dual-Doppler lobe. It included several convective centers lining up on the north-south direction with radar reflectivity over 40 dBZ. The main cells had an east-west extension of 20-30 km. At 1.5 km, the system-relative flow in the line was from front to rear. The inflow was stronger in the main cells at a speed of 5-6 m s^{-1}. Considering the moving speed of the squall line at 5 m s^{-1} on the east-west direction, this front to rear flow matched the weak westerly flow shown at 850 hPa in the environmental sounding (Fig. 2). In other words, the system generated flows at the low levels were mainly along the system. The low-level inflow exhibited a remarkable deceleration at the rear edge of the squall line. This also formed a strong low-level convergence.

Instead of having a narrow ribbon of vertical velocity maximum near the leading edge as the usual squall line, this system had a low-level updraft in a wider rear region. Moreover, the shape of the updraft zone was relatively irregular. In addition to the cellular shaped updraft band at the rear portion, there were elongate updraft band partially crossing the line. The magnitude of the updraft at 1.5 km was up to 3.3 m s^{-1}. The position of the maximum vertical velocity was at about the same location of maximum radar reflectivity. Downward motion up to 2 m s^{-1} was observed in the front portion of the system and between the main convective cells. This also indicated a descending rear to front flow.

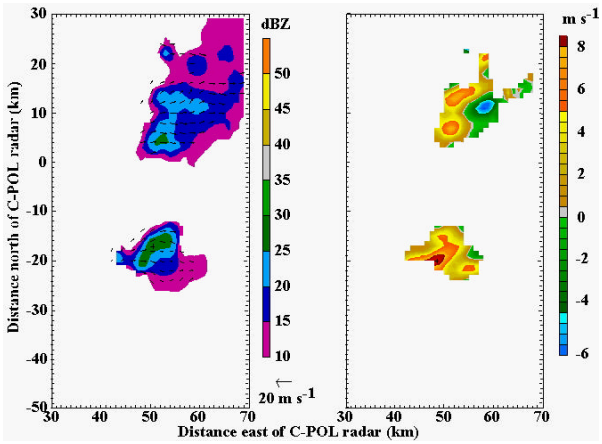

Fig. 5 Same as Fig. 4, except for 9.0 km MSL.

Only the two principal cells of the squall line reached the 9 km MSL with radar reflectivity up to 30 dBZ (Fig. 5). The eastward shift of the cells from the low level indicated an eastward sloping updraft. The airflow was from rear to front, in the opposite direction of low-level inflows. The shape of the updraft was more cellular with maximum vertical velocities of 8 m s^{-1}. The convective downdraft was also evident in the front portion of the cell.

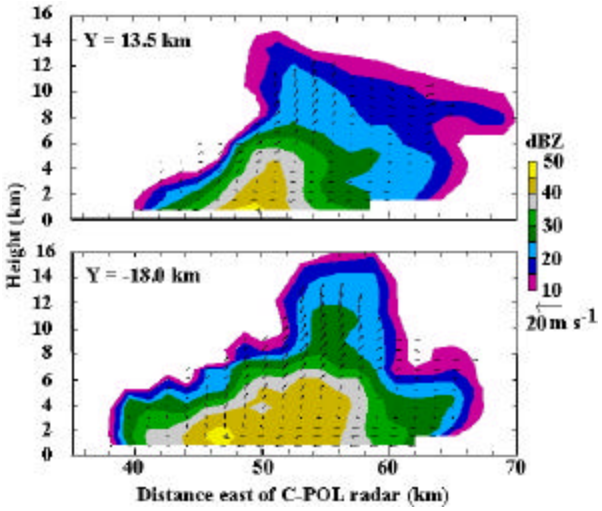

Fig. 6 Vertical cross section of radar reflectivity and line-normal system-relative wind along the lines shown in Fig. 4.

The vertical cross sections of radar reflectivity and vertical velocity across the two main cells are shown in Fig. 6. The cloud top, represented by 10-dBZ reflectivity line, reached 14-16 km MSL. Although not shown in our interpolation, the actual maximum radar reflectivity recorded was about 55 dBZ. The deceleration of the low-level inflow from the front portion was evident in the rear part of the squall line. The convergence generated by this deceleration formed a strong convective center in the place. A tilt of roughly 40° from the horizontal was seen in both the vertical airflow and reflectivity contours in the cross section. It is interesting to note that in this strong convective line, there was little stratiform precipitation associated with it. The environmental sounding taken at 1200 UTC (Fig. 2) clearly showed that the upper level air was very dry. As pointed out in the earlier modeling studies, the dry air in the mid- to upper-levels may result in a quick evaporation of the stratiform cloud after the passage of its convective counterpart. Therefore, no long lasting stratiform rain with larger area coverage was observed on 24 May. From the vertical cross section across the northern cell, there was a nose of weak reflectivity area at around 8 km MSL ahead of the leading edge of the score line. This indicated the tendency of stratiform rain ahead of the system. In a recent climatological studies, Parker and Johnson (2000) found that the leading stratiform cases is only counted for 19% of convective lines observed in the United States, while the trailing or paralleling stratiform rain happen over 80%. A case study on TOGA COARE squall line by Jorgenson *et al.* (1997) also implied that the trailing stratiform rainfall is more common in the tropical squall lines. The investigation on the mechanism responsible for the rear to front mid- to upper-level airflow and its associated leading stratiform rain observed in this case is underway.

4. SUMMARY

Comparing to the tropical squall lines observed in other regions, this narrow squall line system had some interesting features including: 1) with maximum reflectivity as high as 60 dBZ, this convective line has little stratiform rainfall. This may be attributed to the very dry air and weak wind in the upper levels; 2) the low-level inflow was from front to rear, while the upper level outflow was on the opposite direction from rear to front; 3) the small area of stratiform rain was ahead instead of trailing to the convective line; and 4) rather than a narrow ribbon of vertical velocity maximum near the leading edge, this system has an elongate vertical velocity maximum across the system.

Acknowledgements: This research was supported by the NASA under grant NAG5-9699.

REFERENCES

Jorgenson, D. P., M. A. Lemone, S. B. Trier, 1997: Structure and evolution of the 22 February 1993 TOGA COARE squall line: aircraft observations of precipitation, circulation and surface energy fluxes. *J. Atmos. Sci*., **54**, 1961-1985.

Parker, M. D. and R. H. Johnson, 2000: Organizational modes of midlatitude mesoscale convective systems. *Mon. Wea. Rev.*, **128**, 3413-3436.